New Channels in the Reaction Mechanism of the Atmospheric Oxidation of Toluene

ARTICLE *in* THE JOURNAL OF PHYSICAL CHEMISTRY A · AUGUST 2000

Impact Factor: 2.69 · DOI: 10.1021/jp993678d

4 AUTHORS, INCLUDING:

Isidoro García-Cruz
Instituto Mexicano del Petroleo
35 PUBLICATIONS **385** CITATIONS
SEE PROFILE

Alfonso Hernandez-Laguna
Instituto Andaluz de Ciencias de la Tierra
101 PUBLICATIONS **936** CITATIONS
SEE PROFILE

New Channels in the Reaction Mechanism of the Atmospheric Oxidation of Toluene

Victor Hugo Uc,[†] Isidoro García-Cruz,[‡] Alfonso Hernández-Laguna,[§] and Annik Vivier-Bunge*[,§]

Departamento de Química, Universidad Autónoma Metropolitana, Iztapalapa, 09340 México, D.F. Programa de Simulación Molecular, Instituto Mexicano del Petróleo, 07730 México, D.F. Estación Experimental del Zaidín (CSIC), C/Prof. Albareda n1, 18008 Granada, Spain

Received: October 14, 1999; In Final Form: May 22, 2000

Two different theoretical approaches are used to study the OH radical attack on toluene: the Møller−Plesset perturbation theory and the B3LYP density functional method. The critical points of the potential energy surface for the OH addition to toluene are determined, and rate−equilibrium relationships are discussed. A stable structure corresponding to a prereactive complex which is formed when the OH radical is at about 2.5 Å from toluene is obtained. The existence of this loosely bound system is necessary to explain the experimentally observed negative activation energy. The geometry of transition states and products are determined for addition at different positions in the ring, including the ipso position, which has not been considered in previous works. Energy results at the MP4 and coupled cluster levels calculated at the optimized MP2 and B3LYP geometries confirm that the ipso adduct is more stable than the ortho adduct by about 0.5 kcal/mol. Several routes are proposed for the subsequent reactions of the ipso adduct, which could explain the very high yield of *o*-cresol with respect to the other cresol isomers.

1. Introduction

Aromatic hydrocarbons represent about 20% of all the organic compounds emitted to the atmosphere. Of these, toluene is, by far, the most abundant. It is well-known that its initial reaction in the troposphere involves, almost exclusively, the $OH^{\bullet}$ radical[1] via two possible pathways: the abstraction of a hydrogen atom from the side chain to form a benzyl radical and water

$$ArH + OH^{\bullet} \rightarrow Ar^{\bullet} + H_2O \qquad (1)$$

and the addition of the OH radical to the ring

$$ArH + OH^{\bullet} \rightarrow ArH(OH)^{\bullet} \qquad (2)$$

The kinetics and mechanisms of the $OH^{\bullet}$ radical reaction with toluene has been reviewed and evaluated by Atkinson.[2,3] A description of its unusual Arrhenius plot is discussed by Finlayson in ref 1.

The rate of OH decay for toluene was first recorded by Perry et al.[4] over the temperature range 296−473 K at a total pressure of about 100 Torr of argon. As the temperature is increased from about 298 K, the following characteristics are observed:

At room temperature, the OH radical decay is exponential, with the rate constant decreasing slightly as the temperature is increased, thus presenting a positive slope in an Arrhenius plot of log k against $1/T$. For temperatures between 325 and 380 K, the OH decay is no longer exponential and an abrupt change is observed both in the value and in the sign of the slope. For temperatures above 380 K the OH decay is, again, exponential, with a negative slope of the Arrhenius plot.

The highly curved Arrhenius plots have been explained by the competition of the two possible pathways, reactions 1 and 2, whose relative importance varies with temperature. The H-atom abstraction pathway (reaction 1) is of relatively minor importance at room temperature and atmospheric pressure, with $k_1/(k_1 + k_2)$ being approximately equal to 0.1.[4,5]

In order to explain the apparent negative activation energies observed at the lower temperatures, several authors[4−6] have suggested that, in the addition reaction, (2), a prereactive stable π complex could be formed as the reactants approach, prior to the transition state and to the irreversible formation of a σ adduct:

$$ArH + OH^{\bullet} \leftrightarrow [ArH\cdots OH^{\bullet}] \rightarrow ArH(OH)^{\bullet} \qquad (3)$$

In particular, Singleton and Cvetanovic[6] have proposed the following equations derived for a mechanism such as the one in eq 3 at high pressures. If k_f and k_r are the rate constants for the forward and reverse reactions of the first step, respectively, and k_b corresponds to the second step, a steady state analysis leads to a rate constant for the overall reaction which can be written as

$$k = \frac{k_f k_b}{k_r + k_b} \qquad (4)$$

Even though the energy barrier for k_r could be about the same size as that for k_b, the entropy change is much larger in the reverse reaction than in the formation of the products. Thus, one can expect k_r to be considerably larger than k_b. With this assumption, first considered in ref 6, one obtains

$$k = \frac{k_f k_b}{k_r} = \left(\frac{A_f A_b}{A_r}\right) e^{-(E_f + E_b - E_r)/RT} \qquad (5)$$

[†] Universidad Autónoma Metropolitana.
[‡] Instituto Mexicano del Petróleo.
[§] Estación Experimental del Zaidín.

10.1021/jp993678d CCC: $19.00
Published on Web 08/01/2000

where the *A*'s are the preexponential factors. Since E_f is zero, the net activation energy for the overall reaction is

$$E_a = E_b - E_r = (E_{TS} - E_{P-R}) - (E_{reactants} - E_{P-R}) = E_{TS} - E_{reactants} \quad (6)$$

where TS is the transition state and P-R is the prereactive complex. Thus the final expression for E_a turns out to be the usual expression for the calculation of any activation energy, regardless of the energy of the prereactive complex, and, if E_{TS} is smaller than $E_{reactants}$, the activation energy is negative.

In the addition reaction (2), several products are produced,[1,7,8] depending on the reaction conditions. In the first step, the addition adducts are formed, which, in the presence of molecular oxygen and NO_x, yield hydroxyl aromatic compounds, 2-, 4- (see refs 9 and 10), and 3-NO_2 -toluene,[5] and shorter oxidation products such as glyoxal, methylglyoxal, butenedial, etc., which result from the cleavage of the ring.[1,7,8] Of the hydroxyl aromatic compounds, *o*-cresol is the most abundant.

The variation of the overall reactivity of various aromatics toward reaction with the OH radical has been correlated with the nature and position of the substituent groups on the aromatic ring, indicating that electrophilic ring addition is the dominant reaction pathway.[11] In toluene, OH can in principle add to the ortho, meta, or para positions, and also to the carbon atom of the ring which is attached to the methyl group (C_1). The relative rates of OH attack at each ring position for toluene have been investigated by Kenley[5] in a discharge flow system at total pressures of 6−12 Torr and 298 K. An analysis of the cresols in the products led Kenley to establish the following positional selectivity, given in percent of ring addition at each position:

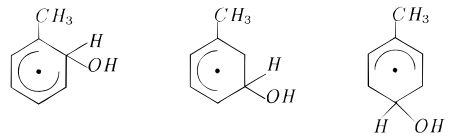

I II III

80.6% 5.1% 14.3%

Since no cresol can be obtained from addition at C_1, the possibility of the formation of the ipso adduct is not included in these percentages.

According to well-known rules of organic chemistry concerning electrophilic addition to aromatic rings, one would expect addition to occur only at the para and ortho positions, with a slight preference for the para, in view of the steric hindrance of the methyl group at the ortho position. The observed preference for attack at the ortho position of toluene by factors of 5.6 and 15.8 with respect to the para and meta positions, respectively, is significantly greater than the statistical preferences and has not been explained.

Theoretical work on the oxidation reactions of aromatic hydrocarbons is scarce. Bartolotti and Edney[12] used a simple density functional approach with the local exchange correlation functional, developed by Vosko−Wilk−Nusair,[13] to identify potential intermediates produced in the OH addition initiated atmospheric photooxidation of toluene. Although their energy results were admittedly preliminary in nature, their calculations were able to confirm certain aspects of the proposed reaction mechanism[2,3] and to predict the importance of carbonyl compounds containing epoxide structures. More recently, Andino et al.[14] performed very extensive and complete theoretical work on the atmospheric oxidation of toluene, *m*- and *p*-xylenes, 1,2,4-trimethylbenzene, and *m*-ethyltoluene. These authors used a combination of semiempirical (PM3) and density functional theory (using the hybrid B3LYP functional[15] to calculate the energies and structures of all the postulated intermediates and products along several possible pathways, up to the final products. In both of these papers[12,14] only the pathways following the OH addition at the ortho position were considered.

In a previous paper on the selectivity of OH addition to xylenes[16] using MP2 and B3LYP calculations, we found a significant contribution from adducts corresponding to addition of the OH radical to C_1. The possibility of addition at the ipso position, however, has not been considered in general, except for *o*-xylene, and the various proposed mechanisms do not mention channels arising from the ipso adducts. For *o*-xylene, several authors[7,18,19] propose schemes for the reaction of the ipso adduct to explain the observed ring cleavage final products, in particular, the observed formation of biacetyl.[18] Yet, as discussed by Traynham,[20] numerous examples of ipso free-radical substitution have been reported, indicating that attack at an already substituted position is likely in free-radical aromatic reactions, just as it is in nucleophilic and electrophilic ones. Moreover, semiempirical calculations[21] indicate that, in free-radical reactions, the ipso intermediate is often the one of lowest energy.

In this work, perturbation theory and density functional methods are used jointly to study the critical points of the potential energy surface (PES) for the OH initial attack on toluene. Previous work performed in our group[16,17] indicates that it is interesting to use these two basically different approaches simultaneously to help in the obtaining of the optimized structures and to better evaluate the results. Energies and geometries of the prereactive complex, and of the transition states and products, are obtained for addition at all four different positions in the ring. Rate−equilibrium relationships are derived.

2. Computational Methodology

Electronic structure calculations have been performed with the system of programs Gaussian94 (G94).[22] Restricted Hartree−Fock theory (RHF) is used for closed shell systems and unrestricted Hartree−Fock theory (UHF) for open shell systems (radicals). The correlation energy corrections are introduced both with Møller−Plesset perturbation theory up to second order (MP2) and with density functional theory using the B3LYP hybrid functional.[15] All geometries have been fully optimized with both methods using a 6-31G** basis set. Energy results from spin-projected MP2 calculations are used (PMP2). The frequency calculations have been performed at the same level as the optimizations. The character of the transition states is confirmed by the existence of only one negative frequency corresponding to the correct transition vector.

Selected calculations have also been performed with higher level methods, namely MP4//MP2/6-31G**, CCSD//MP2/6-31G** and CCSD//B3LYP/6-31G**, to confirm the position selectivity.

The topology of the charge density, $\rho(r)$, has been studied using a Bader analysis at the MP2 level to identify critical points in internal hydrogen bonds and electrostatic interactions.[23,24] The critical points of $\rho(r)$ are classified according to the three canonical curvatures, λ_i, of the Hessian matrix ($H_{ij} = \partial^2\rho(r)/\partial i\,\partial j$, $i, j = x, y, z$). Bond critical points are represented by (3,−1), meaning two negative and one positive curvatures different from zero. They are saddle points of $\rho(r)$. Ring critical points are identified as (3,+1), corresponding to one negative and two

TABLE 1: PMP2/6-31G and B3LYP/6-31G** Total Energies (in hartrees) and MP2 $\langle S^2 \rangle$ Values Before and After Projection, of All the Systems Involved in Reaction 2 for Toluene + OH[a]**

system	PMP2	S^2(before) S^2(after)	ν_i(MP2)	B3LYP	ν_i(B3LYP)
OH	−75.535 371	0.750		−75.728 473	
		0.750			
toluene	−270.692 288	0		−271.578 778	
		0			
P-R complex	−346.233 604	0.761			
		0.750			
i-TS	−346.225 056	1.339	−638	−347.312 621	−299
		1.06			
o-TS	−346.225 670	1.330	−649	−347.315 204	−268
		1.05			
m-TS	−346.223 377	1.342	−676	−347.312 247	−323
		1.06			
p-TS	−346.223620	1.338	−668	−347.313 125	−303
		1.06			
i-OH adduct	−346.257 167	1.1401		−347.338 283	
		0.8472			
o-OH adduct	−346.256 185	1.137		−347.340 582	
		0.846			
m-OH adduct	−346.253 164	1.134		−347.337 878	
		0.845			
p-OH adduct	−346.253 540	1.138		−347.338 86	
		0.847			

[a] The imaginary frequencies (in cm^{-1}) at the transition states have been calculated at both levels. TS stands for the transition state of reaction 2, the P-R complex is the prereactive complex, and the OH adducts are the hydroxymethylcyclohexadienyl radicals with the OH added to the ipso-, ortho-, meta-, and para-carbon atoms.

TABLE 2: Total Energies (in hartrees) of the Ortho and Ipso Adducts, Calculated with Single Point PMP4 and CCSD Methods Using a 6-31G Basis Set**

system	PMP4//MP2	CCSD//MP2	CCSD//B3LYP
o-adduct	−346.360 915	−346.294 424	−346.293 885
i-adduct	−346.361 711	−346.294 825	−346.294 324

positive curvatures. The EXTREME program[25] has been used to determine the critical points of $\rho(r)$.

3. Results

Our present study investigates the reactants, the prereactive complex, the transition states, and the products along four possible reaction paths in the OH radical + toluene addition reaction. The total PMP2 energies of the MP2/6-31G** optimized geometries and the B3LYP/6-31G** energies are given in Table 1. Also given in this table are the $\langle S^2 \rangle$ values before and after projection of higher spin states for the MP2 calculations. It is seen that contamination by higher spin states is especially important with this method, both at the transition states and in the OH adducts, and that states with multiplicity higher than 4 still contribute a little. The corresponding $\langle S^2 \rangle$ values for the B3LYP calculations are not given: they are, in general, about 0.78 before projection and very close to 0.75 after projection. Imaginary frequencies (ν_i) characterizing the transition states and obtained at the corresponding level are also reported in Table 1.

The total energies of the ortho and ipso OH adducts calculated with single point MP4 and coupled cluster methods are given in Table 2.

Reaction energies obtained using the PMP2, B3LYP, PMP4, and CCSD energies of Tables 1 and 2, and calculated with respect to the energies of the reactants, are given in Table 3, together with the experimental results obtained by Perry et al.[4]

The activation energies calculated using eq 6 are reported in Table 4.

From the energies of the adducts of toluene an estimate of the predicted statistical occurrence of the isomers at 298 K can, in principle, be obtained from the classical expression:

$$\% k = \frac{\omega_k e^{-E_k/RT}}{\sum_i \omega_i e^{-E_i/RT}} \quad (7)$$

using the relative energies of the adducts. These estimates are given in Table 5. However, in irreversible exothermic reactions in which no interconversion between the isomers is expected to occur, the selectivity may be kinetic in nature and depend on the height of the activation barriers and on the preexponential factors in the rate constants. In the present reaction, considering that, in the high pressure limit, the prereactive complex has the possibility to stabilize, all the channels have a positive effective transition state barrier. Hence, the relative yields of the different isomers could be calculated using an equation similar to eq 7,

TABLE 3: Reaction Energies (in kcal/mol) for the OH Addition Reaction, Calculated from PMP2, B3LYP, PMP4//MP2, and CCSD//MP2 Energies[a]

system	PMP2	B3LYP	PMP4//MP2	CCSD//MP2
ipso	−19.65	−19.47	−18.00	−9.57
ortho	−19.03	−20.91	−17.50	−9.32
meta	−17.13	−19.21		
para	−17.37	−19.83		

[a] The experimental ΔH_{298} obtained by Perry et al.[4] is −16.5 ± 5 kcal/mol. No isomers are specified.

TABLE 4: Activation Energies (in kcal/mol) for the OH Addition Reaction, Calculated from PMP2 and B3LYP Energies Using Eq 6[a]

system	PMP2	B3LYP
ipso	0.50	−3.36
ortho	0.11	−4.99
meta	1.56	−3.13
para	1.40	−3.68

[a] The reported experimental results range between −0.4 and −1.6 kcal/mol determined at temperatures between 213 and 325 K.[26] No isomers are specified.

TABLE 5: Predicted Percentage of Statistical Occurrence, at 298 K, of the OH−Toluene Isomers, as Obtained from the PMP2 and B3LYP Reaction Energies Using Eq 7[a]

system	PMP2	B3LYP	experiment
ipso	56.8	3.7	
ortho	40.3	84.5	80.6
meta	1.6	4.9	5.1
para	1.2	6.9	14.3

[a] The experimental results of Kenley et al.[5] are indicated in the last column. They do not include the ipso adduct.

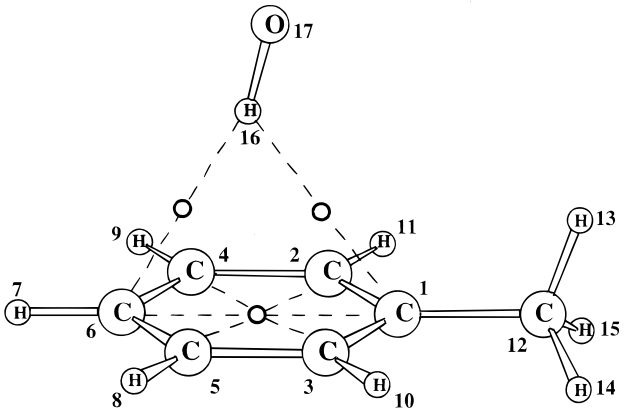

Figure 1. Optimized geometry of the prereactive complex. The circles indicate the position of the critical points of the charge density.

replacing ω by the product of ω times the partition function of the transition state of each isomer, and the E's by the activation barriers. These results are given in the Discussion.

The relevant geometrical parameters of the prereactive complex are indicated in Figure 1 and given in full in Table 6. The critical points of the charge density in the prereactive complex are also indicated in Figure 1, and its bond distances and the topological characteristics of the charge density are given in Table 7. A diagrammatic sketch of the PES for the addition adducts is shown in Figure 2. In Figures 3 and 4, the transition states and their corresponding OH adducts are represented for the ipso and ortho isomers.

4. Discussion

The Prereactive Complex. As the reactants approach each other, a decrease in energy is observed first, and a shallow minimum, corresponding to the prereactive complex is located, whose energy is 4.86 kcal/mol below reactants at the PMP2/6-31G** level. The existence of such minima was already observed by Sosa and Schlegel[27] for the system OH−ethene, and by Diaz-Acosta et al.[28] for OH−propene and for OH−propene−O_2 when the reactants are separated by about 2.7 Å.

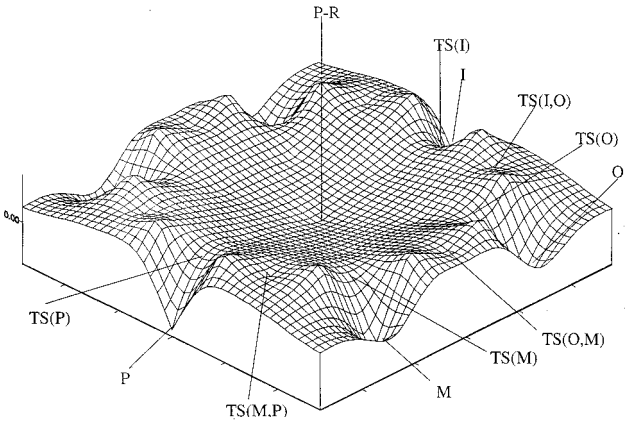

Figure 2. Potential energy surface sketch of the hydroxyl radical addition to toluene (P-R stands for the prereactive complex; I, O, M, and P indicate the critical points for each isomer). The vertical axis is the potential energy; the x and y axes indicate the coordinates of the phenyl group, with the origin at the center of the ring.

The geometry of the prereactive complex is shown in Figure 1. In this system, which has C_s symmetry, the OH radical is seen to be approaching the aromatic ring from above, H first, and at a distance of 2.22 Å from the center of the aromatic ring. The O−C distances with respect to the ipso, ortho, meta, and para carbon atoms are 3.41, 3.44, 3.52, and 3.55 Å, respectively. It is interesting to point out that the OC_1 distance is the shortest. The OH radical is not fully perpendicular to the ring, being a little bent toward C_1, possibly due to a weak interaction between the oxygen and the perpendicular hydrogen of the methyl group. A frequency calculation performed at the MP2/6-31G** level yields a low vibrational frequency at 32 cm^{-1}, which corresponds to a rotation of the OH group so as to decrease the distance between the oxygen atom and C_1. The difference in energy between the isolated reactants and this complex is 4.86 kcal/mol, a value which is similar to that of a weak hydrogen bond.

Two (3,−1) bond critical points of the charge density are found between the H of the OH radical and the C_1 and C_6 carbon atoms (see Figure 2 and Table 7). Their electron density is, as expected, much lower than the one at the C−H (3,−1) bond critical points, and even lower than for a normal hydrogen bond or van der Waals interaction.[23,24] The maximum curvatures, λ_1 and λ_2, are very small. They are similar to, for example, the values of the van der Waals bonds in the Ar···HF complex,[23,24] indicating the presence of a small charge concentration in the direction perpendicular to the bonds. As a consequence, the $\nabla^2\rho$ values present positive signs, corresponding to closed shell interactions in the complex. No (3,−1) bond critical points are

TABLE 6: MP2/6-31G Geometrical Parameters of the Prereactive Complex[a]**

parameter		parameter		parameter	
$r(C_1C_2)$	1.4015	$A(C_3C_1C_2)$	118.3542	$D(C_2C_1C_{12}H_{13})$	88.9573
$r(C_2C_4)$	1.3964	$A(C_1C_2C_4)$	120.9809	$D(C_2C_1C_{12}H_{14})$	−151.2193
$r(C_4C_6)$	1.3974	$A(C_2C_4C_6)$	120.0732		
$r(C_1C_{12})$	1.5056	$A(C_4C_6C_5)$	119.5379		
$r(C_2H_{11})$	1.0839	$A(C_2C_1C_{12})$	120.8073		
$r(C_4H_9)$	1.0826	$A(C_1C_2C_{11})$	119.3702		
$r(C_6H_7)$	1.0824	$A(C_2C_4H_9)$	119.8430		
$r(C_{12}H_{13})$	1.0909	$A(C_4C_6H_7)$	120.2302		
$r(C_{12}H_{14})$	1.0891	$A(C_1C_{12}H_{13})$	110.9651		
$r(O_{17}H_{16})$	0.9728	$A(C_1C_{12}H_{14})$	111.0182		
$r(C_1H_{16})$	2.6973	$A(C_1H_{16}O_{17})$	132.0959		

[a] The structure has a symmetry plane which contains C_{12}, C_1, C_6, H_7, H_{16}, H_{13}, and O_{17}. The ring is practically planar.

TABLE 7: Bond Distances and Topological Characteristics of the Charge Density, $\rho(r_c)$, at the Critical Point of the Bonds and Ring in the Prereactive Complex

	r	r_c[a]	λ_1	λ_2	λ_3	ϵ	$\rho(r_c)$	$\nabla^2\rho(r_c)$
C_1-C_2	1.4015	0.7007	−0.634	−0.520	0.328	0.218	0.307	−0.826
C_2-C_4	1.3964	0.6980	−0.640	−0.524	0.324	0.223	0.309	−0.840
C_4-C_6	1.3974	0.6985	−0.639	−0.524	0.324	0.221	0.309	−0.839
C_1-C_{12}	1.5056	0.7658	−0.485	−0.472	0.337	0.029	0.255	−0.619
C_2-H_{11}	1.0839	0.6787	−0.750	−0.737	0.452	0.018	0.285	−1.036
C_4-H_9	1.0826	0.6785	−0.755	−0.743	0.453	0.017	0.286	−1.046
C_6-H_7	1.0824	0.6782	−0.755	−0.743	0.452	0.017	0.286	−1.046
$C_{12}-H_{13}$	1.0909	0.6810	−0.716	−0.710	0.453	0.008	0.278	−0.973
$C_{12}-H_{15}$	1.0891	0.6785	−0.722	−0.715	0.453	0.009	0.280	−0.984
$H_{16}-O_{17}$	0.9728	0.1922	−1.840	−1.760	1.535	0.045	0.362	−2.064
C_1-H_{16}	2.6973	1.6849	−0.006	−0.001	0.038	6.231	0.008	0.029
C_6-H_{16}	2.5950	1.6448	−0.006	−0.001	0.038	6.231	0.008	0.029
ring			−0.015	0.085	0.091		0.021	0.161

[a] The origin is the first atom indicated in the first column.

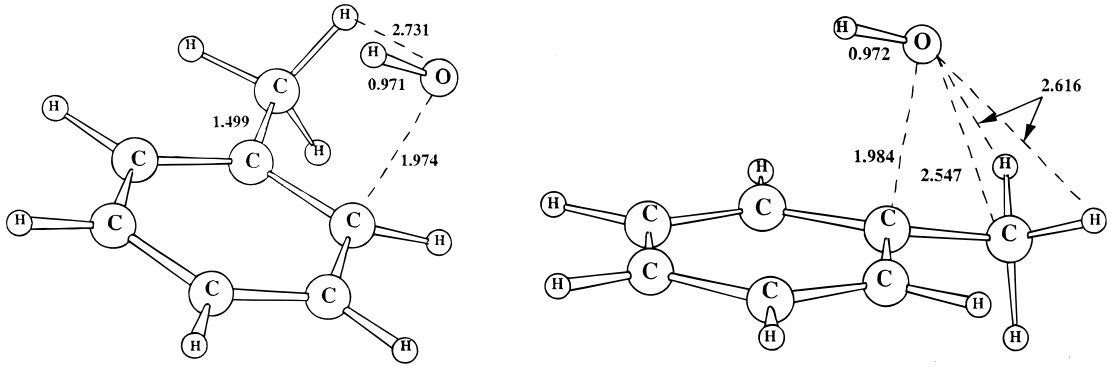

Figure 3. MP2 optimized geometries of the ortho (a) and ipso (b) transition states.

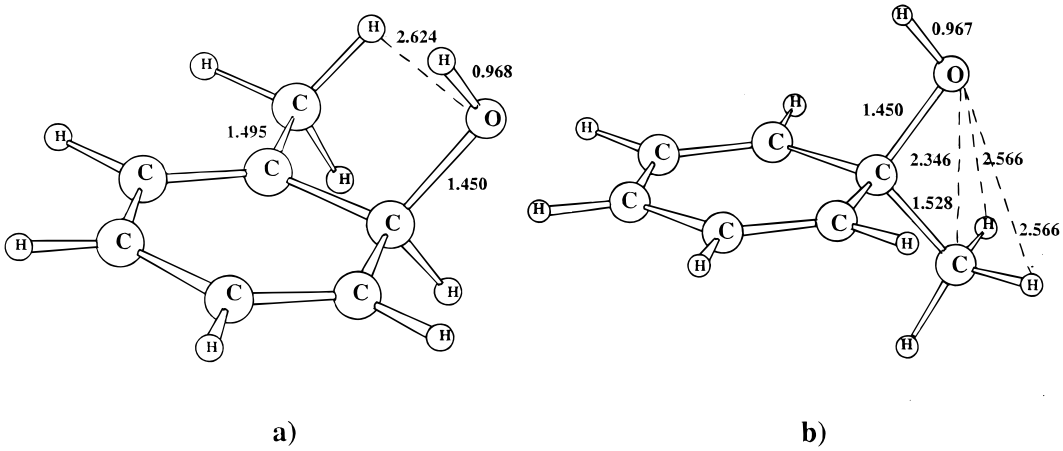

Figure 4. MP2 optimized geometries of the ortho (a) and ipso (b) OH adducts.

found between the oxygen atom and any one of the hydrogen atoms of the methyl group, nor with any of the other carbon atoms.

The structure of this prereactive complex may be considered to be similar to those produced in the equivalent complexes in the first members of the alkene series,[27,28] and it may be compared with cation π complexes.[29] However, in the latter, when a cation is involved in the formation of the π complex, a low energy three-center orbital is formed as a combination of the π orbital and the empty orbital of the cation, with the π orbital participating as a dative orbital, and a very stable π complex is obtained, whose energy may be as much as 60 kcal/mol lower than reactants. In the OH radical addition to π orbitals, however, the dative orbital cannot perform the same role, and the extra electron has to be included in an orbital with antibonding or nonbonding character. Thus, in the OH radical−alkene,[27,28] OH radical−toluene, and OH radical−xylenes series[16] low stabilization energies (of about a few kcal/mol) occur.

In the alkene prereactive complexes, the H of the OH radical points toward the center of the π orbital, at the center of the C═C bond. At this point, which is a (3,−1) critical point, the electron density is a minimum along the bond and a maximum in the directions perpendicular to the bond. In the OH−toluene π complex, the H atom of the OH radical is directed toward the center of the phenyl ring, which is a (3,+1) critical point, a point where the electron density distribution presents a minimum in the plane of the ring and a maximum in the

direction perpendicular to the plane.[23,24] The position of the two (3,−1) critical points between the hydrogen atom of the OH radical and the C_1 and C_6 carbons, which are detected in the prereactive complex, could indicate that a three-center orbital is formed, similar to those in diborane,[23] albeit with an electron density too small to obtain a ring or cage critical points. As expected, a (3,+1) ring critical point is also found at the center of the phenyl ring.

The prereactive complex can be considered as the precursor structure for all addition reactions (ipso, ortho, meta, and para adducts). It is a shallow minimum at the center of the PES and it constitutes a branching out point for all the addition channels (Figure 2).

The OH + Toluene Addition Reactions. Six transition structures (Figure 2) are found surrounding the prereactive complex on the PES, leading to the six different isomers of the hydroxytoluene adducts. Coming from the prereactive complex, the OH radical appears to flip toward the ring, positioning itself in a configuration nearly parallel to the ring, with the oxygen atom pointing to the nearest reactive carbon. The ortho transition state (TS) has the lowest energy, 4.98 kcal/mol above the prereactive complex. From this point, the reaction proceeds to form the ortho derivative and finally the *o*-cresol, as found in the experiments. The second TS, in order of increasing energy, corresponds to the one at the ipso position, at 5.36 kcal/mol. The methyl steric hindrance is probably responsible for the slightly higher energy of this structure. The oxygen is nearer to the methyl hydrogens than in the ortho TS (see Figure 3), and more separated from the reactive carbon. The other two transition state structures, meta TS and para TS, are higher in energy than the previous ones, with the para TS a little lower than the meta TS.

When the PMP2 results are analyzed, it is observed that none of the four transition state energies is lower than the energy of the isolated reactants (Table 5), so that the negative activation energies detected in the experiments are not very well reproduced by these calculations. The PMP2 ortho TS and ipso TS, however, present activation energies which are only 0.1 and 0.5 kcal/mol above the reactants, respectively. The B3LYP results present the right sign (Table 5). However, the PMP2 activation energies are closer to the range of the available experimental results (−0.4 to −1.6 kcal/mol determined at temperatures between 213 and 325 K).[26] Contrary to most ab initio methods, and Møller−Plesset in particular, B3LYP is known to underestimate the height of reaction barriers.[30]

As for the transition vectors in the transition states, they correspond to the deformation of the ring, with the O atom moving toward the carbon atom involved in the bond and the OH group remaining approximately parallel to the plane of the rest of the ring.

Concerning the adducts, the ipso isomer is found to be more stable, by only 0.5 kcal/mol, than the ortho isomer, if energy values calculated at either PMP2 or PMP4/6-31G** levels are used (Table 3). However, at the B3LYP/6-31G** level, the ipso derivative is less stable than both the ortho and the para isomers. Additional single point coupled cluster calculations performed at the MP2/6-31G** and the B3LYP/6-31G** optimized geometries to try to resolve the discrepancy yield the following result: in both cases, the ipso isomer is found to be more stable than the ortho isomer by 0.25 kcal/mol. However, the MP2 geometries are clearly the ones yielding the lowest CCSD energies.

It is interesting to note that the reaction energies obtained from the projected MP*n* and from DFT results agree rather well with the experimental results (Table 3 and ref 4). Coupled cluster reaction energies, however, are only about half the value obtained with the other methods. Two reasons may be advanced to explain this discrepancy. On the one hand, the CCSD results for the adducts present a large spin contamination, with $\langle S^2 \rangle = 1.13$, and results for projected coupled cluster calculations are not available. On the other hand, the latter are performed without geometry optimization. The interest for performing these calculations in this work concerns the possibility of helping decide on the relative stability of the ortho and ipso isomers.

The oxygen atom of the ipso adduct is at a distance of 2.35 Å from the carbon of the methyl group. The high stability of this isomer could conceivably arise from the interaction of the lone pairs of the oxygen with the hydrogen of the methyl group in a star conformation (see Figure 4). In the ortho adduct, the methyl group changes to an eclipsed conformation in order to allow a hydrogen atom to interact with a lone pair of the oxygen (Figure 4), at a distance of 2.55 Å.

In fact, the preference for addition of OH at the ipso position is not surprising: it is equivalent to that observed in addition reactions at double bonds, the latter favoring the most substituted carbon atom. It is in line with the experimental and theoretical results presented by Traynham.[20] In the case of propene, MP2 calculations[28] have indeed shown that the favored addition product is the one with OH located at the central carbon atom. We have recently recalculated the energies of the OH adducts of propene, using the B3LYP/6-31G** method with full geometry optimization: as in the case of toluene, the relative stability of both isomers is reversed.

Several routes can be proposed for the subsequent reactions of the ipso adduct. First, phenol could be formed, and it should then be found in an important amount, in the same way that cresols do, following identical oxidation channels. Phenol is indeed found, albeit in minor amounts.[8] We suggest that the ipso-hydroxytoluene adduct may undergo a 1,2 OH shift, perhaps catalyzed by molecular oxygen attacking the hydrogen of the hydroxyl group. This reaction would also explain the observed relatively high yield of 80.6% *o*-cresol at 298 K.[5] A similar 1,2 rearrangement has been shown to occur to an appreciable extent when *p*-bromonitrobenzene is photochlorinated. According to Traynham,[20] the identification of rearrangement of an ipso substituent to an ortho position may account for the high proportion of ortho substitution that is characteristic of many free-radical aromatic substitution reactions.

As obtained from our PMP2 results, the theoretical populations estimated for a thermodynamically controlled reaction are 56.8%, 40.3%, 1.6%, and 1.2%, at 298 K, for the ipso, ortho, meta, and para adducts, respectively (Table 5). If the populations are calculated without considering the ipso adduct, the para isomer presents a very low yield in comparison with the experimental yield. Although the para adduct is more stable than the meta isomer, possibly due to the inductive effect of the methyl group, the population of the meta derivative is slightly higher due to the degeneration degree of the meta positions. The inductive effect also plays an important role in lowering the energy of the ortho isomer.

It is not surprising that the corresponding percentages obtained using eq 7 and the B3LYP energies are in much better agreement with experimental results, since this method gives very little weight to the ipso adduct. If a kinetic control is assumed, and the data for the available MP2 partition functions of the transition states are used, the results are not satisfactory: 57.9%, 11.5%, 22.0%, and 8.5%, at 298 K, for the ipso, ortho, meta, and para adducts, respectively.

Kenley et al.[5] obtained only 3-NO_2-toluene in the reaction of *o*-cresol with NO_2. However, other authors[8−10] also obtained very small quantities of 2- and 4-NO_2-toluene. The 2-NO_2-toluene could come from the ipso adduct. The channel from the ipso adduct to 2-NO_2-toluene should be more reactive than the channel to phenol, so phenol would be obtained only in minor quantities.

Even considering the possibility that the stability of the ipso derivative is exaggerated in the PMP*n* and CCSD calculations, and that the internal interactions with the oxygen lone pairs are overestimated, it is clear that the formation of the ipso adduct is not negligible, and that it should yield detectable concentrations of certain products, as observed, for example, in the *m*- and *p*-cresols. In particular, the ipso adduct could produce oxidation products derived from the cleavage of the ring, such as methylglyoxal and butenedial[7,8] by a mechanism similar to the one suggested by Shepson et al.[7] for the oxidation of *o*-xylene. Indeed, calculations performed on the OH adducts of *o*-xylene[16] have shown, unequivocally, that the ipso adduct is strongly favored.

Finally, we would like to suggest that the ipso adduct may also be somehow related to the formation of benzaldehyde. The latter is obtained in considerable amounts, and it has always been assumed that it is a product formed in the hydrogen abstraction channel (eq 1). However, we have shown[31] that the barrier for the direct abstraction of a hydrogen atom from the side chain of toluene, to form a benzyl radical and water, is relatively high, of the same order as the one for the abstraction of a primary hydrogen in alkanes. Further work is needed on this subject.

Rate−Equilibrium Relationships. It is interesting to look for possible relationships, in the form of linear and quadratic equations, between the equilibrium energies of the adduct isomers and their transition state energies. In the following discussion the PMP2 energies have been used.

A plot of $\Delta E^{\#} = E_{P-R} - E_{TS}$ as a function of $\Delta E = E_{P-R} - E_{adduct}$ (where E_{P-R}, E_{TS}, and E_{adduct} are the total energies of the prereactive complex, the transition states, and the adducts, respectively) for all the isomers does not yield a linear relationship. The ipso isomer, however, may have to be considered apart from the others, since it is the only one for which the OH radical has to overcome the methyl steric effect. Indeed, if the ipso adduct is removed from the series, a good linear fit is obtained:

$$\Delta E^{\#} = 15.8 \pm 0.17 + (0.76 \pm 0.01)\Delta E$$

which has a correlation coefficient $r^2 = 1.0000$ and a standard deviation s.d. = 0.0195 with energies in kcal/mol. The equation above corresponds to a Bell−Evans−Polanyi model[32,34] and to a Leffler equation.[33] The physical meaning of the fitting parameters might be the following:

(i) The intercept is the value of the barrier for $\Delta E = 0$ reaction. It can be considered either as a integration constant (Leffler's model[33]) or as the intrinsic reaction barrier ($\Delta E_0^{\#}$) of the series (as in Marcus' theory[35]). The concept of an intrinsic barrier is well-known in Marcus' theory[35] as applied to electron transfer reactions,[35] proton transfer reactions,[36,37] alkyl transfer reactions,[38] and S_N2 reactions,[34,39] but in the OH$^{\bullet}$ addition reactions to toluene the physical meaning of the intrinsic barrier is not clear. $\Delta E_0^{\#}$ for the addition reaction could be the barrier to go from a prereactive critical point on the upper face of toluene to one on the opposite face. A schematic energy path leading over the intrinsic barrier between the ortho and meta positions is represented in Figure 5. In this figure, the ortho and meta paths are projected on the plane of the intrinsic reaction path.

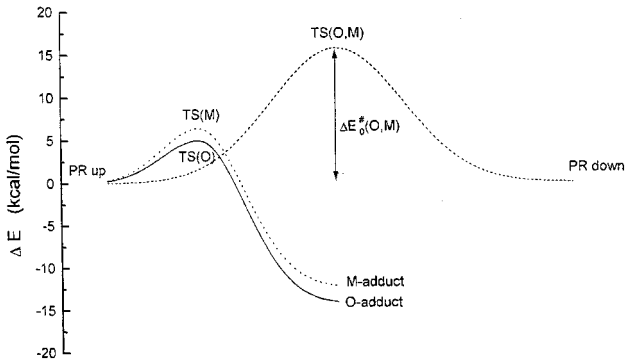

Figure 5. Schematic energy paths: Solid line, P-R → ortho adduct; dashed line, path leading over the intrinsic barrier from the face-up P-R to the face-down P-R; doted line, P-R → meta adduct.

The nuclear configuration of the transition state ($TS_0^{\#}$) could be one in which the OH radical is in the plane of the phenyl ring. Unlike the transfer and S_N2 reactions mentioned above, the intrinsic reaction barrier of the OH addition to toluene would have to have a reaction coordinate different than those of the addition isomers. Whereas the reaction coordinates leading to the adducts point approximately toward the carbon atoms of the phenyl group, those of the thermoneutral reactions bisect the C−C bonds. Since the thermoneutral reactions can proceed along a path which goes either between the ortho and meta positions or between the meta and para positions, two slightly different ($TS_0^{\#}$)'s should exist with a perceptible energy difference between them. Thus, the energy of the intrinsic reaction barrier could be taken to be the average between both values:

$$\Delta E_0^{\#} = (1/2)(\Delta E_0^{\#}(o,m) + \Delta E_0^{\#}(m,p))$$

In the present case, the value obtained for the intrinsic barrier (15.8 kcal/mol) is similar, with the opposite sign, to the reactioin energies (which lie between −17 and −19 kcal/mol depending on the isomer) and approximately 3 times the value of the addition barriers (5.0, 6.4, and 6.3 kcal/mol for the ortho, meta, and para adducts, respectively). The transition state $TS_0^{\#}$ belongs to the PES of the addition reactions, since it is the high barrier nearest the addition barriers. It determines the neighboring critical points, such as the addition TSs in the formation of the ortho, meta, and para adducts (see Figures 2 and 3).

(ii) The slope has the physical meaning of the Brønsted parameter, α.[34] This parameter is also related to the Leffler−Hammond principle,[33,34,40] and it can be interpreted as a measure of the relative position of the transition state on the reaction coordinate. Its value should range between 0 and 1 (1 − α indicating the closeness between the transition states and the reactants).[33] In this reaction α is a constant equal to 0.76, suggesting that all the transition states should be closer to the products than to the reactants. Indeed, taking the C···O distance as the main internal variable in the reaction coordinate, its MP2 value is 3.44 Å in the prereactive complex, 1.97 Å in the TSs, and 1.45 Å in the adducts.

If the energy data corresponding to the ortho, meta, and para addition channels are fit to the Marcus equation[34,35,39]

$$\Delta E^{\#} = \Delta E_0^{\#} + \frac{1}{2}\Delta E + \frac{1}{16\Delta E_0^{\#}}\Delta E^2$$

a fair fit is obtained. However, if the intercept and the coefficient of the linear term in the previous equation are allowed to adjust freely, the following relation is obtained:

$$\Delta E^{\#} = 16.5 \pm 0.18 + (0.86 \pm 0.01)\Delta E + \frac{1}{(16)(16.5)}\Delta E^2$$

with $r^2 = 1.0000$ and s.d. $= 0.0206$. Thus, statistical parameters similar to those of the linear fit are obtained. In fact, both the height of the intrinsic barrier (16.5 kcal/mol), which is similar to the one obtained in the linear fit, and the very small coefficient of the quadratic term (0.004) explain why the relationship is almost linear. The coefficient of the linear term is slightly different from 0.5, the value in the Marcus equation. Considering

$$\alpha = \frac{d\Delta E^{\#}}{d\Delta E}$$

in the previous fit,[34] we obtain the following equation:

$$\alpha = 0.86 + \frac{\Delta E}{(8)(16.5)}$$

which yields 0.75, 0.77, and 0.76 for the ortho, meta, and para TSs, respectively. All of these values fall within a narrow interval and indicate that the TSs should be more similar to the adducts than to the prereactive complex.

One can conclude that the ortho, meta, and para addition reactions follow a quasi Marcusian behavior; the deviation could be due to the existence of different reaction coordinates for the thermoneutral reaction.

If the ipso reaction is included in the set of data, fitting via the Marcus equation is not satisfactory. However, if the four sets of data are adjusted to a quadratic polynomial, the following equation is obtained:

$$\Delta E^{\#} = 103.3 \pm 33.5 + (14.04 \pm 5.0)\Delta E + (0.5 \pm 0.2)\Delta E^2 \quad (8)$$

with $r^2 = 0.9998$ and s.d. $= 0.175$. Both statistical parameters are better than those obtained with the Marcus equation, the coefficient of the linear term is much larger than the 1/2 value of the Marcus equation, and the intercept goes up to 103.3 kcal/mol, indicating a very high $\Delta E_0^{\#}$(i,o). Indeed, the reaction path near the methyl group should have a very high intrinsic barrier, due to the steric hindrance of this group. The α values are found to be -0.75, 0.16, 1.74, and 1.54 for the ipso, ortho, meta, and para isomers, most of them being outside of the $0-1$ interval.[34] The ipso TS would be the one least similar to the products. In this case, the behavior is not of the Marcus type at all.

5. Conclusions

Several methods based on a different approach to electron correlation have been used in this work to study the formation and the relative stability of the four OH−toluene isomers. The ipso adduct is considered here for the first time. It is found that the PMP*n* and the CCSD methods attribute a much greater stability to the ipso adducts than B3LYP, inverting its relative importance as a product of the OH + toluene addition reaction.

The reaction energies agree rather well with experiment except for the CCSD results, which present considerable spin contamination in the adducts, and it cannot be projected out. The large spin contamination also observed in the MP*n* calculations is certainly a drawback. Using projected MP*n* results approximately corrects these deficiencies. Also, the activation energies obtained with this method are not negative, as expected. However, for the ortho and the ipso isomers, the calculated activation energies are close to zero. The two problems mentioned above do not occur with B3LYP. As already observed in other DFT calculations on other types of systems,[14,16] DFT does yield negative activation energies. However, there are other deficiencies in this method; i.e., the negative barriers are, in general, much too low (in fact, in work recently performed on OH hydrogen abstractions from alkanes,[30] barriers are also found to be negative, which is definitely not correct), and the interactions between the oxygen atom and the methyl group in ipso additions are given very little weight. The combined use of these two approaches, and the fact that results are in reasonable agreement, should lend credibility to the trends described in this work.

A prereactive structure has been found, in which the OH radical is bound to the aromatic ring by two weak interactions characterized by two (3,−1) bond critical points of the charge density. The prereactive complex can be considered as the precursor structure for all the addition reactions.

The specific interaction responsible for the extra stability of some isomers with respect to others appears to be the interaction of the lone pairs on the oxygen atom with hydrogen atoms from neighboring methyl groups, the latter clearly rotating in order to shorten the O···H distances involved. In the case of the ipso adduct, two lone pairs on the oxygen atom interact with two hydrogen atoms of the methyl group attached to C_1. The distance between these atoms is about 2.57 Å.

New results have been obtained in this work, concerning, in particular, the stability of the OH adduct corresponding to the OH addition at the ipso position of the ring. Even considering the possibility that the stability of the ipso derivative is exaggerated in the PMP*n* and CCSD calculations, it is clear that the formation of this adduct is not negligible, and that it should yield detectable concentrations of certain products, as observed, for example, for the meta and para isomers. Moreover, the energy barrier for its formation from the prereactive complex is found to be quite low. The question that remains to be discussed concerns the fate of this adduct, which has not been considered in experimental work. In this work, three schemes are suggested: (i) the ipso-hydroxytoluene adduct may undergo a 1,2 OH shift, (ii) it may lead to the formation of 2-NO_2-toluene, and (iii) it could produce oxidation products derived from the cleavage of the ring, such as methylglyoxal and butenedial.

Rate−equilibrium relationships suggest the possible existence of intrinsic barriers which would be an integral part of the PES. They would be the high barriers nearest the transition state structures in the different channels of addition, contributing a constant kinetic factor to the thermodynamic driving force of the $OH^{\bullet}$ addition reactions in toluene.

The ortho, meta, and para series follows an equation similar to the Marcus equation, with a nearly constant Brønsted parameter, α. The deviation from the Marcus equation can be due to the existence of different reaction coordinates leading to the intrinsic barriers and to the adducts. The height of the intrinsic barrier is quite close to the equilibrium energies, and approximately 3 times the size of the reaction barriers. When the ipso derivative is included in the series, the behavior of the series and the interpretation of the intrinsic reaction barrier are less clear.

Acknowledgment. The authors gratefully acknowledge financial support from the Instituto Mexicano del Petróleo

through Program FIES-95-97-VI, from Grant PB97-1205 of the Spanish DGES, and from Conacyt through Project 400200-5-25482E, and the computing time on the Silicon Graphics Origin 2000 at the Universidad Nacional Autónoma de Mexico (UNAM) in Mexico City.

References and Notes

(1) Finlayson-Pitts, B. J.; Pitts, N. *Atmospheric Chemistry: Fundamentals and Experimental Techniques*; Wiley Interscience: New York, 1986; p 6.

(2) Atkinson, R. *J. Phys. Chem. Ref. Data* **1989**, *Monogr. 1*, 1.

(3) Atkinson, R. *J. Phys. Chem. Ref. Data* **1994**, *Monogr. 2*, 1.

(4) Perry, R. A.; Atkinson, R.; Pitts, J. N. *J. Phys. Chem*. **1977**, *81*, 296.

(5) Kenley, R. A.; Davenport, J. E.; Hendry, D. G. *J. Phys. Chem.* **1981**, *85*, 2740; *J. Phys. Chem*. **1978**, *82*, 1095.

(6) Singleton, D. L.; Cvetanovic, R. J. *J. Am. Chem. Soc.* **1976**, *98*, 6812.

(7) Shepson, P. B.; Edney, E. O.; Corse, E. W. *J. Phys. Chem*. **1984**, *88*, 4122.

(8) Dumdei, B. E.; O'Brien, R. J. *Nature* **1984**, *311*, 248.

(9) Lonneman, W. A.; Seila, R. L.; Bufaline, J. J. *Environ. Sci. Technol*. **1978**, *12*, 459.

(10) Fritz, D. R.; Grosjean, D.; van Cauwenbergher, K.; Pitts, J. N., Jr. *Photooxidation Products of Toluene-NO_x Mixtures under Simulated Atmospheric Conditions*. Presented at the 175th National Meeting of the American Chemical Society, March, 1978.

(11) Ravinshankara, J. M.; Wagner, S.; Fisher, S.; Smith, G.; Schiff, R.; Warson, R. T.; Tesi, G.; Davis, D. D. *Int. J. Chem. Kinet*. **1978**, *10*, 783.

(12) Bartolotti, L. J.; Edney, E. O. *Chem. Phys. Lett*. **1995**, *245*, 119.

(13) Vosko, S. J.; Wilk, L.; Nusair, M. *Can. J. Phys*. **1980**, *58*, 1200.

(14) Andino, J. M.; Smith, J. N.; Flagan, R. C.; Goddard, W. A., III; Seinfeld, J. H. *J. Phys. Chem*. **1996**, *100*, 10967.

(15) Becke, A. D. *J. Chem. Phys*. **1993**, *98*, 5648.

(16) Uc, V. H.; García-Cruz, I.; Vivier-Bunge, A. In *Quantum Systems in Chemistry and Physics*; Hernandez-Laguna, A., et al., Eds.; Advanced Problems and Complex Systems; Kluwer Academic Publishers: Norwell, MA, 2000; Vol. II, pp 241−259.

(17) García-Cruz, I.; Castro, M.; Vivier-Bunge, A. *J. Comput. Chem.* **2000**, *21*, 716.

(18) Darnall, K. R.; Atkinson, R.; Pitts, J. N., Jr. *J. Phys. Chem*. **1979**, *83*, 1943.

(19) Atkinson, R.; Carter, W. P. L.; Winer, A. M. *J. Phys. Chem*. **1983**, *87*, 1605.

(20) Traynham, J. G. *Chem. Rev*. **1979**, *79*, 323.

(21) Eberhardt, M. K.; Yoshida, M. *J. Phys. Chem*. **1973**, *77*, 589.

(22) Frisch, M. J.; Trucks, G. W.; Schlegel, H. G.; Gill, P. M. W.; Johnson, B. G.; Robb, M. A.; Cheeseman, J. R.; Keith, T. A.; Petersson, G. A.; Montgomery, J. A. Raghavachari, K.; Al-Laham, M. A.; Zakrzewski, V. G.; Ortiz, J. V.; Foresman, J. B.; Cioslowski, J.; Stefanov, B. B.; Nanayakkara, A.; Challacombe, M.; Peng, C. Y.; Ayala, P. Y.; Chen, W.; Wong, M. W.; Andres, J. L.; Replogle, E. S.; Gomperts, R.; Martin, R. L.; Fox, D. J.; Binkley, J. S.; Defrees, D. J.; Baker, J.; Stewart, J. P. Head-Gordon, M.; Gonzalez, C.; Pople, J. A. *Gaussian 94*; Gaussian, Inc.: Pittsburgh, PA, 1995.

(23) Bader, R. F. W. *Atoms in Molecules*; Clarendon Press: Oxford, 1990.

(24) Bader, R. F. W. *Chem. Rev*. **1991**, *91*, 893.

(25) EXTREME program, in AIMPAC. Koning, S. W. B.; Bader, R. F. W.; Tang, T. *J. Comput. Chem*. **1982**, *3*, 317.

(26) Baulch, D. L.; Cobos, C. J.; Cox, R. A.; Frank, P.; Hayman, G.; Just, Th.; Kerr, J. A.; Murrells, T.; Pilling, M. J.; Troe, J.; Walker, R. W.; Warnatz, J. *J. Phys. Chem. Ref. Data* **1994**, *23*, 941.

(27) Sosa, C.; Schlegel, H. B. *J. Am. Chem. Soc*. **1987**, *109*, 4193.

(28) Díaz-Acosta, I.; Alvarez-Idaboy, J. R.; Vivier-Bunge, A. I. *J. Chem. Kinet*. **1999**, *31*, 29.

(29) (a) Deward, S.; Dougherty, R. C. *Teoria de las perturbaciones de los OM (PMO) en Quimica Organica*; Reverte: Madrid, 1980. (b) Brown, H. B.; Brady, J. D. *J. Am. Chem. Soc*. **1952**, *74*, 3570.

(30) García-Cruz, I.; Ruíz-Santoyo, M. E.; Alvarez-Idaboy, J. R.; Vivier-Bunge, A. *J. Comput. Chem*. **1999**, *20*, 845.

(31) García-Cruz, I.; Uc, V. H.; Vivier-Bunge, A. Unpublished results.

(32) Ogg, R. A., Jr.; Polanyi, M. *Trans. Faraday Soc*. **1935**, *31*, 604. Evans, A. G.; Evans, M. G. *Trans. Faraday Soc*. **1935**, *31*, 1401. Bell, R. P. *Proc. R. Soc. London, Ser. A* **1936**, *154*, 414. Evans, M. G.; Polanyi, M. *Trans. Faraday Soc*. **1938**, *34*, 11. Evans, M. G.; Warhurst, E. *Trans. Faraday Soc*. **1938**, *34*, 614. Bell, R. P.; Lidwell, O. *Proc. R. Soc. London, Ser. A* **1940**, *176*, 114. Bell, R. P. *J. Chem. Soc., Faraday Trans. 2* **1976**, *72*, 2088.

(33) Leffler, J. E. *Science* **1953**, *117*, 340.

(34) Shaik, S. S.; Schlegel, H. B.; Wolfe, S. *Theoretical Aspects of Physical Organic Chemistry. The S_N2 Mechanism*; John Wiley & Sons, Inc.: New York, 1992.

(35) Marcus, R. A.; Sutin, N. *J. Chem. Phys*. **1956**, *24*, 966 and 979. Marcus, R. A. *J. Chem. Phys*. **1957**, *26*, 867 an 872. Marcus, R. A. *Can J. Chem*. **1959**, *37*, 155. Marcus, R. A. *Discuss. Faraday Soc*. **1960**, *29*, 21. Marcus, R. A. *J. Chem. Phys*. **1963**, *67*, 853. Marcus, R. A. *Annu. Rev. Phys. Chem*. **1964**, *15*, 155. Marcus, R. A. *J. Chem. Phys*. **1965**, *43*, 679. Marcus, R. A.; Sutin, N. *Comments Inorg. Chem*. **1986**, *5*, 119.

(36) Kresge, A. J. *Acc. Chem. Res*. **1975**, *8*, 354.

(37) Albery, W. J. *Annu. Rev. Phys. Chem*. **1980**, *31*, 227.

(38) Albery, W. J.; Kreevoy, M. M. *Adv. Phys. Org. Chem*. **1978**, *16*, 85.

(39) Wolfe, S.; Mitchell, D. J.; Schlegel, H. B. *J. Am. Chem. Soc*. **1981**, *103*, 7692 and 7694.

(40) Hammond, G. S. *J. Am. Chem. Soc*. **1955**, *77*, 334.